Received: 22 July 2022 | Revised: 23 December 2022 | Accepted: 28 December 2022

DOI: 10.1002/hyp.14801

RESEARCH ARTICLE

WILEY

Settling of superparamagnetic silica encapsulated DNA microparticles in river water

Yuchen Tang[1] | Fengbo Zhang[2] | Thom Bogaard[1] | Claire Chassagne[3] | Zeeshan Ali[4] | Sulalit Bandyopadhyay[4] | Jan Willem Foppen[1,2]

[1]Water Resources Section, Department of Civil Engineering and Geosciences, Delft University of Technology, Delft, Netherlands

[2]IHE Delft Institute for Water Education, Delft, Netherlands

[3]Hydraulic Engineering, Department of Civil Engineering and Geosciences, Delft University of Technology, Delft, Netherlands

[4]Norwegian University of Science and Technology, Trondheim, Norway

Correspondence
Yuchen Tang, Water Resources Section, Department of Civil Engineering and Geosciences, Delft University of Technology, 2628 CN Delft, Netherlands.
Email: y.tang-3@tudelft.nl

Funding information
China Scholarship Council; Nederlandse Organisatie voor Wetenschappelijk Onderzoek, Grant/Award Number: STW14515

Abstract

Particle tracers are sometimes used to track sources and sinks of riverine particulate and contaminant transport. A potentially new particle tracer is ~200 nm sized superparamagnetic silica encapsulated DNA (SiDNAFe). The main objective of this research was to understand and quantify the settling and aggregation behaviour of SiDNAFe in river waters based on laboratory settling experiments. Our results indicated, that in quiescent conditions, more than 60% of SiDNAFe settled within 30 h, starting with a rapid settling phase followed by an exponential-like slow settling phase in the three river waters we used (Meuse, Merkske, and Strijbeek) plus MilliQ water. In suspensions of 1000× higher particle concentrations, the hydrodynamic diameter ($D_{h\text{-}DLS}$) of SiDNAFe increased over time, with its polydispersity index (PDI) positively correlated with particle size. From these observations, we inferred that the rapid SiDNAFe settling was mainly due to homo-aggregation and not due to hetero-aggregation (e.g., with particulate matter present in river water). Incorporating a first-order mass loss term which mimics the exponential phase of the settling in quiescent conditions seems to be an adequate step forward when modelling the transport of SiDNAFe in river injection experiments. Furthermore, we validated the applicability of magnetic separation and up-concentration of SiDNAFe in real river waters, which is an important advantage for carrying out field-scale SiDNAFe tracing experiments.

KEYWORDS
aggregation, DNA tracer, microparticle, settling

1 | INTRODUCTION

Engineered particles in the nanometre or micrometre size range, like metal particles, plastics, or rubbery fragments, in riverine ecosystems have received increasing attention due to their potential ecotoxicological effects (Hochella et al., 2019; Kooi et al., 2018; van Emmerik et al., 2019; van Emmerik & Schwarz, 2020). Tracer tests can improve our understanding of particulate transport in these rivers (Leibundgut & Seibert, 2011). For the past two decades, researchers have been exploring synthetic DNA strands for environmental tracing (Dahlke et al., 2015; Foppen et al., 2013; Mahler et al., 1998; Sabir et al., 1999). Over the last several years, a microparticle labelled with synthetic DNA was developed (Paunescu et al., 2013; Sharma et al., 2012). These DNA-tagged microparticles are generally featured by synthetic DNA strands being encapsulated or protected by an external coating (Garnett et al., 2009; Liao et al., 2020; McNew

et al., 2018; Pang et al., 2020; Paunescu et al., 2013; Sharma et al., 2012). Compared with traditional solute/particulate tracers, such as fluorescent dyes/microspheres, DNA-tagged tracers enable true multi-tracing with their engineered identical surface properties but unique synthetic DNA signatures, allowing a theoretically unlimited number of distinguishable tracer varieties without environmental interference. Later, superparamagnetic DNA-tagged silica microparticles (SiDNAFe MPs) were designed with a magnetite core in order to facilitate easy harvesting and up-concentration from larger volumes of sample water (Puddu et al., 2014; Sharma et al., 2021).

These SiDNAFe MPs are expected to behave like colloidal particles, whereby DLVO theory can be used to interpret findings (Petosa et al., 2010; Praetorius et al., 2020). Homo-aggregation and hetero-aggregation of nano/micro-particles were studied in the presence and/or the absence of natural organic matter (NOM) and suspended particulate matter (SPM) of varied types and concentrations in relevant freshwater conditions (e.g., Abe et al., 2011; Domingos, Ju-nam, et al., 2009; Domingos, Tufenkji, & Wilkinson, 2009; Liu et al., 2011; Metin et al., 2014; Oncsik et al., 2014; Ottofuelling et al., 2011; Quik et al., 2013; Zhao et al., 2021). Homo-aggregation was shown to be quantitatively unimportant at realistic environmental concentrations and relevant time scales, yet hetero-aggregation was considered as a more important mechanism given the higher concentrations of natural colloids and SPM (Labille et al., 2015; Lead et al., 2018). Overall, driving factors in particle hetero-aggregation in rivers mainly were pH, ionic strength, the presence of divalent ions, and the type/concentration of NOM and SPM (Baalousha et al., 2016; Buffle et al., 1998; Klaine et al., 2008; Lagarde et al., 2016; Zhang et al., 2009).

Particle settling is considered to be an important process in freshwater systems, representing a downward energy/nutrient/contaminant flux from the water column to the benthic environment. Of particular interest are the settling of riverine SPM (e.g., fine and coarse organic particulate matter), engineered nano/micro particles, and potentially their co-settling (Hoellein et al., 2019; Hünken & Mutz, 2007; Kumar et al., 2021; Vincent & Hoellein, 2021). Riverine SPM is mainly composed of macro- and micro-aggregates/flocs of inorganic and biogenic colloidal particles, organized by bacterial exopolymeric substances (EPS) (Lartiges et al., 2001; Many et al., 2016). The high surface area to volume ratio and high organic content of SPM is conducive to interactions with other colloids and substances (Newbold et al., 2005; Ongley et al., 1992). Consequently, SPM settles differently from the settling of its constituent particles. It is difficult to use Stokes' law to predict the settling velocity of SPM, due to the various single-aggregate densities over the spectrum of SPM sizes (Khelifa & Hill, 2006; Larsen et al., 2009). The resultant settling of SPM is a collective of contributing factors, such as structural characteristics, bulk densities, the effect of NOM and thus the flocculation potential (Lee et al., 2019; Zimmermann-Timm, 2002). For example, enhanced SPM flocculation was found in nutrient-rich (e.g., EPS) water conditions, where aggregates were formed with significantly larger sizes (Tang & Maggi, 2016). Nevertheless, the settling velocities of SPM aggregates were found mostly invariant and ranged between 1 and 4 mm/s in natural river environments across a wide range of density, size and organic matter fraction (Maggi & Tang, 2015).

For engineered nano/micro particles (ENP), given the practical limitations of quantifying aggregation-settling processes in real natural environments, most studies focused on the settling in quiescent conditions, to understand either enhanced or diminished settling as a result of hetero-aggregation or stabilization (Klaine et al., 2008; Lagarde et al., 2016; Petosa et al., 2010; Quik et al., 2010, 2012, 2013). Results from those static settling experiments could be used to obtain important parameters (e.g., hetero-aggregation and sedimentation rate) for modelling the exposure concentration of nano/micro particles in large rivers (Besseling et al., 2017; Garner et al., 2017; Praetorius et al., 2012; Quik et al., 2015). Usually, co-settling experiments of ENP with NOM (e.g., EPS) and SPM employ higher than realistic concentrations to observe the co-settling due to strong hetero-aggregation. However, weak hetero-aggregation, such as a small amount of ENP adsorption on cell surfaces, may have detrimental effects on organisms (Ma et al., 2015). SiDNAFe particles could be an alternative for studies on potential ecotoxicological effects of extremely low concentrations of ENP in natural environment.

Sedimentation could be an important removal mechanism for SiDNAFe MPs which would jeopardize its application as particulate tracer. Encountering naturally occurring material, such as SPM, SiDNAFe MPs would likely undergo aggregation and subsequent settling, which could alter the transport and fate of the SiDNAFe MPs in aqueous conditions. For example, the sedimentation rate of dispersed nano/microparticles in the presence of SPM was found to be significantly higher than those without (Li et al., 2019; Velzeboer et al., 2014). Reduced transport of nano/micro-particles could result from a high attachment efficiency to SPM, where the resultant aggregates are subject to gravitational sedimentation due to increased size and density (Petosa et al., 2010; Shevlin et al., 2018). Thus, the settling potential of SiDNAFe MPs in real river waters in quiescent conditions needs to be investigated before their release in rivers, which is of practical importance when employed in future tracing applications. In this regard, the main objective was to understand and quantify the settling behaviour of SiDNAFe MPs, by conducting a series of settling experiments with filtered and non-filtered natural river waters. This research adds to the current knowledge of such novel hydrological colloidal tracer, providing insights for future development of the DNA-based tracing framework, which could serve as a promising and powerful tool for advancing the knowledge of hydrological processes.

2 | MATERIALS AND METHODS

2.1 | SiDNAFe MPs and DNA analysis

The synthesis of SiDNAFe MPs was described in Sharma et al. (2021). Briefly, synthetic double-stranded DNA (dsDNA) was firstly bound with positively charged iron oxide nanoparticles (IONPs), thereafter, these DNA-tagged IONPs were encapsulated within a silica shell. For DNA analysis, a protocol was followed similar to that described in

Tang et al. (2021). Briefly, to release DNA, the protective silica shell was dissolved by buffered oxide etch solution (BOE). The released (intact) ds-DNA amount was determined by using quantitative polymerase chain reaction (qPCR), whereby the ds-DNA was exponentially amplified and quantified. Prior to DNA analysis, to mitigate inhibition during qPCR, the SiDNAFe MPs were magnetically separated from river water, re-dispersed and up-concentrated in MilliQ water (MQ) (Figure 1).

Zeta potential of the SiDNAFe MPs was measured in filtered river water and in MQ, respectively, by using a Zetasizer (Zetasizer Nano S, Malvern Instr., UK). Hydrodynamic diameter ($D_{h\text{-}DLS}$) of SiDNAFe MPs was obtained by dynamic light scattering (DLS). Distribution algorithm (General Purpose) and cumulant analysis were both used to calculated the $D_{h\text{-}DLS}$ from the measured correlogram. The General Purpose algorithm fitted the exponentially decaying correlogram to a sum over several exponential decay functions that decayed at different rates, achieved by non-negative least squares (NNLS) (Morrison et al., 1985). The results were reported in the displayed size distribution as peaks, each with a characteristic width. In contrast, the cumulant analysis modelled the particle size distribution as a Gaussian, with the average hydrodynamic diameter (Z-Ave) being the mean value and the polydispersity index (PDI) being the variance of the hypothetical Gaussian (Koppel, 1972; Stetefeld et al., 2016). To have good scattered light signals, a SiDNAFe concentration of 10^{-2} mg/ml was used, which was 1000 times higher than the settling experiments (10^{-5} mg/ml). The measurement position was at the centre of the cell with 173° backscattering. The particle size distribution (PSD) of the SiDNAFe MPs suspended in MQ was characterized based on their sedimentation rate in a centrifugal force field by a centrifugal separation analysis using a LUMiSizer (STEP-Technology, L.U.M GmbH, Berlin, Germany). Briefly, the apparatus measures light transmission over the total length of the sample cell containing sample suspension, whereby time dependence of the position of the interface particle-free fluid/particle suspension was determined (Lerche, 2002). These transmission profiles were then transformed into velocity distributions and size distributions given the particle density (see details in the SI).

2.2 | Settling experiments

The settling of the SiDNAFe MPs was recorded by measuring DNA concentration of the supernatant at a fixed depth as a function of time. Filtered (0.45 µm cellulose-acetate filter, MF-Millipore® & 1.2 µm glass microfiber filter (GF/C), Whatman) and unfiltered river water types were used for the settling experiments. The initial concentration (C_0) of the SiDNAFe MP was 10^{-5} mg/ml, which was prepared by diluting the stock tracer solution (1 mg/ml SiDNAFe MPs suspended in MQ) in filtered, in unfiltered river water, or in MQ (as a control). Subsequently, well-mixed suspensions of SiDNAFe MPs were aliquoted in 15 ml PE tubes for separate sample-taking and then allowed to quiescently settle at 4°C (in-situ monitored by a micro temperature/pressure gauge, Van Essen) in a refrigerator for 2, 4, 6, 22, 24, and 30 h. Following the settling for the selected time period, 1 ml of sample was taken with a micropipette from 1 cm (∼±1 mm) below the water surface for sample analysis (Figure 1). In each water type, settling experiments were performed in duplicate. At each time step, SiDNAFe concentration was quantified in duplicate using qPCR. The SiDNAFe settling curve was based on the averaged relative mass concentration C/C_0 with the standard deviation based on four measurements at each time step.

To assess homo-aggregation of SiDNAFe MPs, $D_{h\text{-}DLS}$ of SiDNAFe was measured in MQ at 4°C before, during, and after a 4-h settling experiment, by using dynamic light scattering in a Zetasizer Nano SZ. Additionally, for comparison, the same settling experiment was conducted with SiDNAFe suspended in 5 mM phosphate buffer (0.77 g/L of $Na_2HPO_4{\cdot}7H_2O$) (0.0029 M) (EMSURE®, Merck KgaA, Germany) and 0.29 g/L of $NaH_2PO_4{\cdot}H_2O$ (0.0021 M) (J.T. Baker, Spain) dissolved in demineralized water; pH adjusted to 7.0–7.1 using 100 mM NaOH (J.T. Baker, Poland), in which SiDNAFe was more negatively charged (Chakraborty et al., 2022). To better interpret the DLS measurement results, the same settling experiment was conducted with manually milled silica colloids from silica power of 0.2–0.7 mm (Sigma-Aldrich, Germany, product number: 85356) with an approximate concentration 10 times higher (∼0.1 mg/ml). As a control, $D_{h\text{-}DLS}$

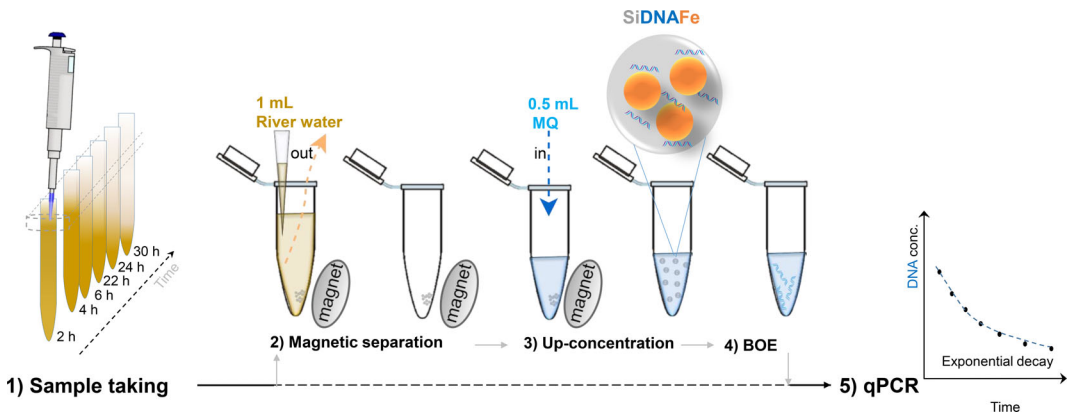

FIGURE 1 A settling experiment including sample analysis. (1) A 1 ml sample was taken from a settling tube; (2) in this sample solution, SiDNAFe MPs were magnetically separated by using an external magnet; (3) SiDNAFe MPs were up-concentrated by adding 0.5 ml MQ; (4) encapsulated DNA was released by adding BOE; (5) DNA concentration was determined using qPCR

was measured right after sample sonication and vortexing prior to the settling experiment. The sample was allowed to settle without disturbance for 4 h, during which $D_{\text{h-DLS}}$ was recorded every 0.5–1 h. After that, final measurements were taken after the sample was gently inverted several times.

2.3 | Calculating settling

In MQ, settling of SiDNAFe MPs with radius r (nm) can be described by Stokes' law (Stokes, 1850), whereby SiDNAFe MPs settled without collision and flocculation in a dilute suspension. The terminal settling velocity of the SiDNAFe MPs with radius i is given by:

$$v_i = \frac{2}{9} \times \frac{\rho_p - \rho_f}{\mu} \times g \times i^2. \quad (1)$$

With $\rho_p - \rho_f$ being equal to the density difference between particles (p) and fluid (f) (kg/m^3), μ the dynamic viscosity (Pa s) of the particle-free suspension medium, g the gravitational constant (m/s^2), and i particle radius (m).

From the water surface (depth $h = 0$) down to any given depth (h) at time (t) (Figure 2), the suspension would be devoid of particles with settling velocity greater than $\frac{h}{t}$ and would contain particles with a settling velocity less than $\frac{h}{t}$. The concentration c at a given h and time t would be the sum of the original concentrations of particles which settle slower than $\frac{h}{t}$:

$$c(h,t) = \sum_{all\ i} \left(c_i | v_i < \frac{h}{t} \right) = \sum_{all\ i} c_{0,i} H_{v_i t}, \quad (2)$$

where, c_i and v_i denote the mass concentration (mg/ml) and the terminal settling velocity (mm/h) of particle size class i, respectively.

At the required time, we took 1 ml of suspension at a fixed depth of the settling column from a slice of water in the settling tube between h_1 and h_2 (Figure 2). Assuming a monodisperse suspension

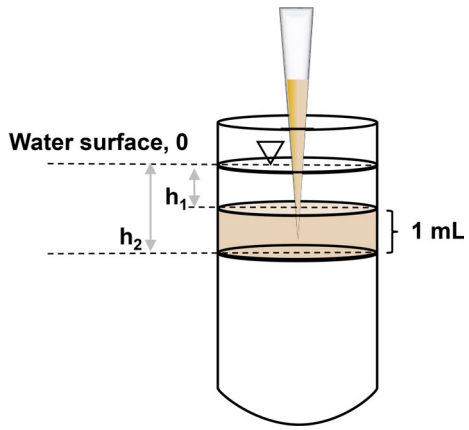

FIGURE 2 Schematic representation of the sampled volume in the numerical simulation

of SiDNAFe MPs with a particle radius i having particle number N_i being in the water column between the water surface 0 and the depth h_2, at any time t, the mass concentration between depth h_1 and h_2, could be described as:

$$c_i(h_1 \sim h_2, t) = \begin{cases} N_i * (h_2 - h_1)/h_2 * V_i * \rho, & v_i * t < h_1 \\ N_i * \dfrac{h_2 - v_i * t}{h_2} * V_i * \rho & h_1 \le v_i * t \le h_2, \\ 0 & \text{otherwise} \end{cases} \quad (3)$$

where, V_i is the spherical volume of a particle with radius i, and ρ is the density of the SiDNAFe MPs. Then, the relative mass concentration, C_R, could be described as:

$$C_R = \sum_{all\ i} c_i(h_1 \sim h_2, t) / \sum_{all\ i} N_i * (h_2 - h_1)/h_2 * V_i * \rho. \quad (4)$$

In addition, the C_R of SiDNAFe MPs was calculated using the measured PSD from the LUMiSizer.

Finally, a best-fit PSD was derived from the observed settling curve, using Genetic Algorithm, available in Python. This algorithm solves an optimization problem based on the mechanics of natural selection, whereby fitting parameters can be automatically improved (Holland, 1992).

2.4 | Characterization of river water

In all, three river water types were collected from different sources, each with differing SPM and organic matter (OM) content. Meuse river water was collected from the river Meuse at Keizersveer, The Netherlands (51°43′05.7″ N, 4°53′27.5″ E). Strijbeek and Merkske water were collected from Strijbeekse Beek (51°29′58.3″ N, 4°47′01.7″ E) and Merkske (51°24′57.1″ N, 4°50′48.5″ E), respectively, which were two small rivers located on the border of the Netherlands and Belgium. River water sampling was carried out on the same day in winter of 2021 (06/01/2021). Upon collecting water samples, iodide was added to reach a concentration of 1 ppm to minimize microbial activity during sample storage. Water samples were kept at 4°C in polyethylene sample containers and completely filled and tightened with double-sealed plastic caps. The OM content of river water was measured as dissolved organic carbon (DOC, in mg-C/L) using the combustion technique with a total organic carbon analyser (TOC-VCPN [TN], Shimadzu, Japan). Electrical Conductivity (EC) and pH were measured in situ using an EC meter and pH meter, respectively. The total suspended solids (TSS) in river water samples were calculated by drying the filtrate (>1.2 μm) at 105°C and weighing the dry weight of the filtrate. Main compositions of SPM (>1.2 μm) in river water samples were identified by using Energy-dispersive X-ray spectroscopy (EDS) with a Scanning Electron Microscope (SEM) (JSM-6010A, JEOL, Tokyo, Japan). In addition, high-resolution images of the SPM were taken by the SEM operated at 20 kV. As proxies for SPM (Velde, 1977; Velzeboer et al., 2014), total Fe and Al were

measured by a PlasmaQuant MS Inductively Coupled Plasma Mass Spectrometry (ICP-MS) (Alanlytik Jena, Jena, Germany). Before ICP-MS measurement, to dissolve SPM completely, river water samples were microwave-digested with 65% HNO_3 using a CEM MARS5 Digestion Oven (CEM corporation, USA).

2.5 | Statistical analysis

Two-sample *t*-test (*p* value <0.05) was used to determine whether there was a significant difference between the settling of the SiDNAFe MPs in natural waters and in MQ. The null hypothesis was that the observed settling in MQ was not significantly different from the settling in river water types.

3 | RESULTS

The SPM presented in the three river waters was negatively charged, with zeta potentials ranging between ∼15.9 and ∼18.6 mV (Table 1), with extremely polydisperse size distributions (results not shown). Elemental analysis showed that Si, Fe and Al were dominant (Figure 3, details on elemental data [%] in the SI). In fact, SPM from the Meuse was an assemblage of heterogeneous aggregates and polymer-like material of various shapes and sizes, where Si, Fe, and Al elements were distributed across the entire frame with no particular pattern. Selected as proxies of the SPM, total Fe and total Al in each river water type were also quantified (Figure 4f). Most SPM mass was found in the size classes smaller than 0.45-µm and larger than 1.2-µm in these three river types. The mass concentration of Fe and Al reduced as the filter size reduced, with the largest Fe concentration decrease (more than 50%) from the unfiltered to 1.2 µm-filtered sample water. Then, from 1.2 to 0.45 µm, Fe and Al concentrations hardly changed. Especially, ∼50% of total Fe and Al originated from the size classes smaller than 0.45-µm in case of Strijbeek and Merkske. Conversely, SPM in Meuse was dominant by inorganic particles larger than 1.2 µm.

Zeta potential of SiDNAFe MPs in the three rivers was similar to that in MQ (∼−22 to −24 mV; Table 1), while the electrical conductivity was in a typical fresh water range (371–543 µS/cm; Table 1). Meuse water had highest TSS (10.4 mg/L) and lowest DOC content (6.0 mg/L), while the other two river water shared similar characteristic with high DOC (∼17.0 mg/L) and low TSS (2.0 mg/L).

We observed that in MQ, ∼40%–50% of the SiDNAFe MP mass concentration rapidly settled out in the first 2–6 h (Figure 4; referred to as 'stage 1' hereafter). Then, from 6 to 30 h, the SiDNAFe MP concentration remained almost constant (referred to as 'stage 2') with a significantly ($p < 0.01$) lower settling rate compared to the first 6 h of settling. The settling behaviour of SiDNAFe in river water resembled that in MQ (Figure 4, Table S3a), whereby we also observed two distinct stages with a significantly different ($p < 0.01$) settling rate, regardless of river water type or filter size. In fact, there was no statistically significant difference ($p > 0.05$) between the settling in MQ ('MQ-obs.' in Table 1) and in river waters (Table 1). In addition, the difference between the two stages was also clear from the size of the error bars, as these were significantly larger for stage 1 settling than for stage 2 settling ($p < 0.05$; Table S3b). Furthermore, the observed settling in all water types was statistically significantly larger ($p < 0.05$) than the expected Stokes' settling, which was derived from the PSD measured by LUMiSizer in MQ (Figure 4 and 'MQ-sim.' in Table 1). This discrepancy was likely due to the rapid settling during stage 1. During stage 2, the SiDNAFe MPs generally followed Stokes' settling, as the subtle decline in concentration from hour 6 to hour 30 visually concurred well with the descending slope of the expected settling curve. Finally, we found a best-fit PSD with a mean radius of 338 nm by fitting the measured settling data (Figure 4e). This mean radius was 3 times larger than the measured mean radius (i.e., 101 nm; Table S2).

The settling experiment of SiDNAFe MP using a 1000× concentrated particle suspension in MQ showed that only one peak was

TABLE 1 Characteristics of water types, the zeta potential of SiDNAFe and *p*-value from *t*-test

	Unit	Meuse	Strijbeek	Merkske	MQ
SiDNAFe ζ	mV	−22.7 ± 3.3	−22.6 ± 3.3	−22.6 ± 3.1	−24.2 ± 3.8
SPM ζ	mV	−16.5 ± 4.4	−18.6 ± 4.4	−15.9 ± 3.5	-
EC	µS/cm	371	491	543	-
DOC	mg/L	6.0	17.0	17.5	0.1
TSS	mg/L	10.4	2.0	2.0	n.a.
pH	mg/L	7.9	7.1	7.3	6.5
p-value (<0.05)					
MQ-obs.	0.45 µm	0.65	0.11	0.12	-
	1.2 µm	0.21	0.76	0.39	
	Non-filtered	0.57	0.45	0.19	
MQ-sim.	0.45 µm	0.0027	0.0018	0.0043	0.0020
	1.2 µm	0.0099	0.0047	0.0014	
	Non-filtered	0.0038	0.023	0.0012	

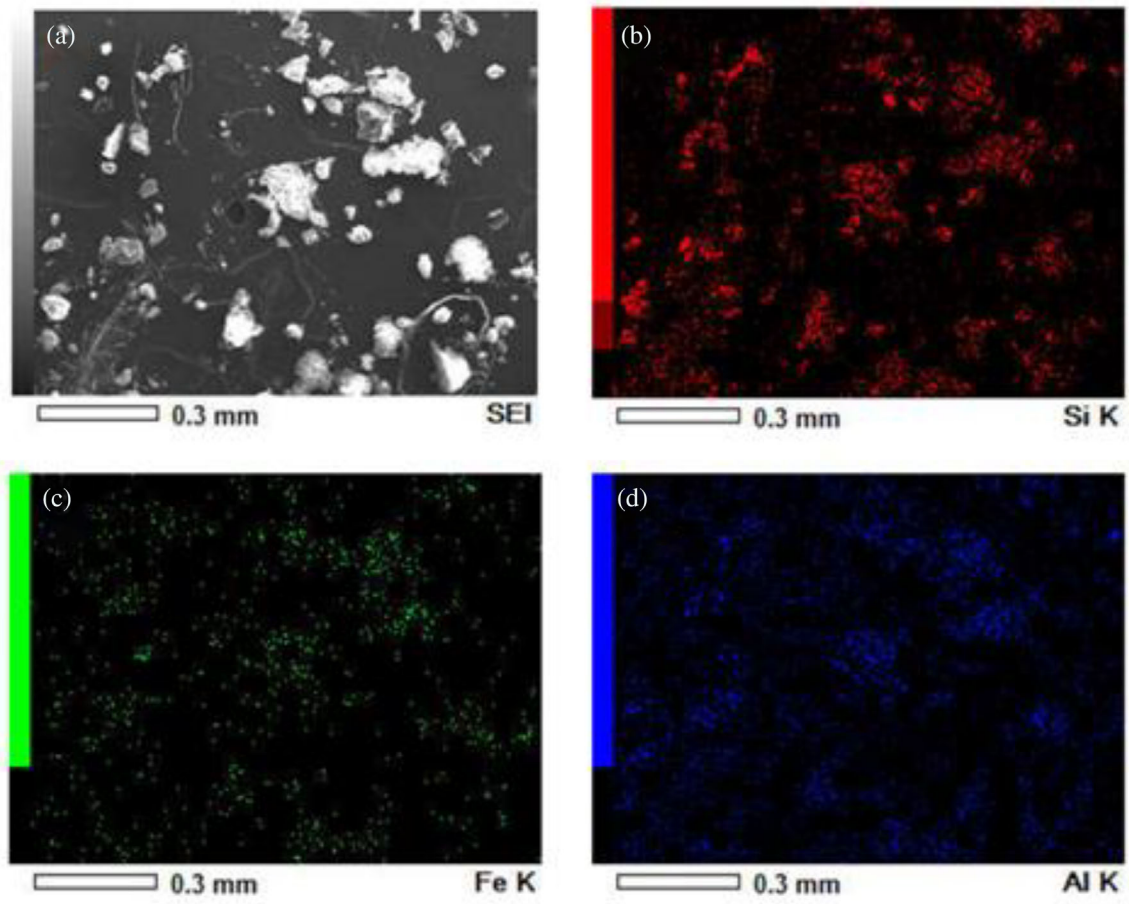

FIGURE 3 Energy-dispersive X-ray spectroscopy (EDS) mapping of dried SPM from Meuse river water, including (a) SEM image, (b) Si element, (c) Fe element, and (d) Al element

visible before settling, while a second peak formed during settling (Figure 5a, upper panel). After the experiment and after inverting the sample, a peak appeared with an almost 8–10 times larger diameter than the one before settling (Figure 5a, the upper panel). Moreover, PDI showed a positive correlation with Z-Ave, with data points initially clustered at a consistent size and gradually scattered as a function of Z-Ave (Figure 5a, the lower panel), indicating aggregation (Malm & Corbett, 2019). For comparison, for SiDNAFe MP suspended in 5 mM phosphate buffer and SiO_2 colloids suspended in MQ, no hydrodynamic diameter change was observed (Figure 5b,c, the upper panel), with well-defined clusters of PDI data indicating colloidal stability (Figure 5b,c, the lower panel).

4 | DISCUSSION

4.1 | Settling of SiDNAFe MPs in MQ

In MQ, we observed two distinct stages (i.e., the fast and the slow stages) of settling. We interpreted the fast settling during stage 1 due to the presence of relatively large aggregates in suspension. Assuming the SiDNAFe MPs were initially completely suspended in MQ with a low volume fraction (a very dilute suspension of $\sim 10^{-5}$ mg/ml), for quiescent conditions, SiDNAFe MPs would have to come close enough to form aggregates through random Brownian motion and/or differential sedimentation, whereby repulsive interparticle and/or hydrodynamic interactions would hinder the approach of colliding particles. Given the small mean diameter of SiDNAFe (i.e., ~200 nm), the collision rate derived from Brownian motion was likely more significant than from differential sedimentation (Elimelech et al., 2013). More specifically, the estimated collision efficiency for perikinetic aggregation was extremely low in the presence of an energy barrier of >30 kBT (see Table S1 in the SI). Under such unfavourable conditions, only one in every million collisions would occur between particles having sufficient energy to overcome the barrier (Elimelech et al., 2013). Based on this reasoning, we speculate that a small portion of aggregates of SiDNAFe MPs were formed due to increased shear force (Johnson et al., 1996; van de Ven & Mason, 1977) during the manual mixing when diluting for different water types prior to the actual settling experiments. Shear-induced aggregation of a similar type of DNA-tagged silica microparticle was also observed and discussed in our previous research (Tang et al., 2021). Moreover, as mentioned before, we observed an increase in the $D_{h\text{-}DLS}$ of SiDNAFe during a 4-h settling experiment using a 1000× concentrated particle

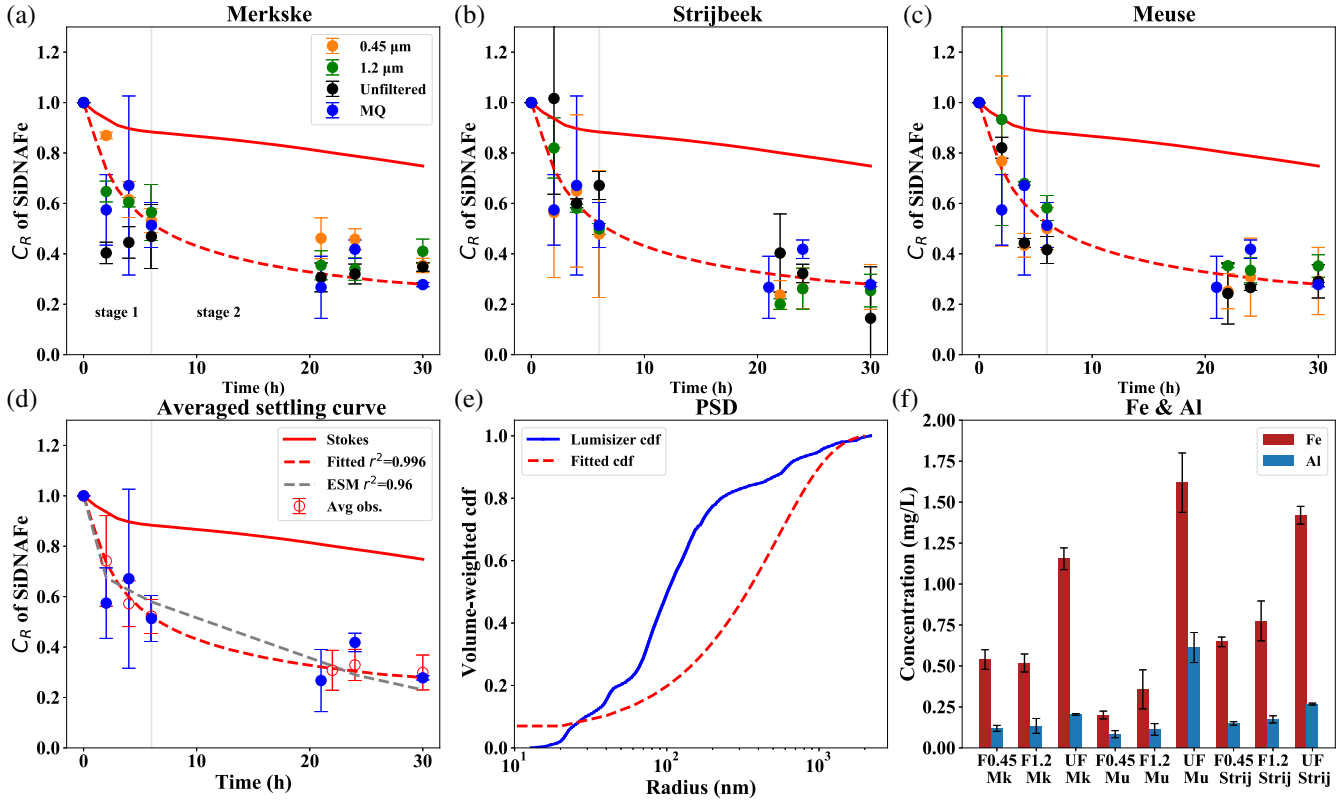

FIGURE 4 (a–d) Settling of the SiDNAFe MPs in MQ and in filtered and unfiltered river water types. The red solid and the red dashed curves delineate Stokes' settling with a PSD measured by LUMiSizer and with a PSD fitted from the observed curve, respectively, while the grey dashed curve represents settling following an exponential settling model. (e) Volume-weighted cumulative size distribution function (cdf) of the SiDNAFe MPs measured by LUMiSizer in comparison with the fitted cdf. (f) Total Fe and total Al as proxies of the SPM in filtered and unfiltered river waters. F0.45, F1.2, and UF: 0.45-µm, 1.2-µm filtered, and unfiltered water; Mk, mu, and Strij: Merkske, Meuse, and Strijbeek, respectively

suspension (10^{-2} mg/ml) in MQ (Figure 5a, the upper panel) compared to the previous settling experiment (10^{-5} mg/ml). From these observations, we inferred that SiDNAFe homo-aggregation had taken place in MQ, whereas no homo-aggregation had taken place when SiDNAFe was more colloidally stable. So, SiDNAFe homo-aggregation was very likely occurring during the sample preparation stage before the settling experiments.

4.2 | Settling in river water

The main elemental compositions of SPM in river waters were Al, Fe and Si, which corresponds to the main inorganic fraction of most riverine SPM aggregates, such as silicate mineral and clay (Slomberg et al., 2016; Wilson et al., 2014). The SPM found in our three river waters were likely aggregates of inorganic particles and debris associated with organic materials, as reported by Lartiges et al. (2001). Coexisting with SPM in river waters, SiDNAFe MPs might hetero-aggregate with SPM, resulting in enhanced settling (Velzeboer et al., 2014; Zhu et al., 2018). Surprisingly, regardless of the filtered/unfiltered river water, SiDNAFe MPs settled identically to the settling in MQ, where hetero-aggregation was absent. From this observation, we inferred that SiDNAFe MPs did not hetero-aggregate with SPM present in these river waters. Foremost, SiDNAFe MPs were negatively charged with similar zeta potentials for the three river waters, exhibiting a relatively high energy barrier (with low collision efficiency, as discussed earlier) and a negligible secondary energy minimum (Table S1). Likewise, SPM found in these three river water types was slightly less negatively charged, which is within the range of zeta potentials reported for most SPM found in freshwater (i.e., −15 to −30 mV; Jekel, 1986; Jerry & Pecoraro, 1996; Kim & Sansalone, 2008; Buffle et al., 1998; Domingos, Tufenkji, & Wilkinson, 2009). For solution chemistry conditions like in the case of natural river water, repulsive interactions such as electrostatic repulsion or steric hindrance would dominate and thus likely hinder the approach between SiDNAFe MPs and SPM (Petosa et al., 2010). In our experiments, a rigorous inspection of the composition and structures of the SPM was beyond the scope. However, we would like to speculate that, compared with SiDNAFe MPs, SPM would probably settle much faster and thus rapidly removed itself from the sampling section. Maggi and Tang (2015) found that SPM in freshwater settled with mostly invariant settling velocities, ranging from 1 to 4 mm/s, across a broad spectrum of density, size and organic matter fraction. This was because of the fractal architecture of SPM, which balanced the increase in floc size and the decrease in effective density. In this regard, we may not overlook the chance of differential settling,

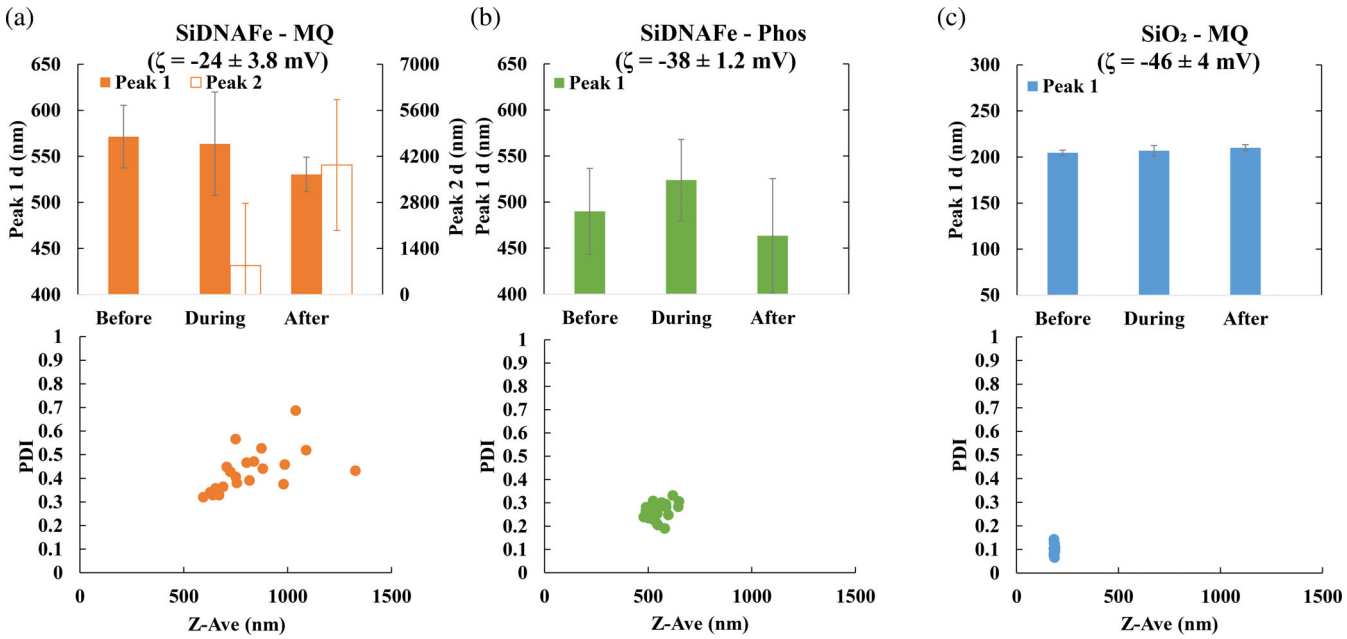

FIGURE 5 Change of mean $D_{h\text{-}DLS}$ over 4 h and Z-Ave as a function of PDI in settling experiments performed in a Zetasizer. (a) SiDNAFe suspended in MQ (zeta potential ζ: −24 ± 3.8 mV); (b) SiDNAFe suspended in a phosphate buffer (ζ: −38 ± 1.2 mV); (c) SiO_2 colloids suspended in MQ (ζ: −46 ± 4 mV). In the upper panel of (a–c), peak 1 and 2 were derived from the General Purpose Algorithm. Peak 1 is the main peak, plotted on the primary *y*-axis; while peak 2, the minor peak, is plotted on the secondary *y*-axis. The error bars are standard deviations of 15 measurements. 'Before', 'During', and 'After' indicate before and during settling, and after inverting the sample at the end of the experiment. In the lower panel of (a–c), Z-Ave and PDI were calculated using the cumulant analysis

whereby collisions occurred when rapidly settling SPM overtook and intercepted SiDNAFe MPs settling more slowly (Lick et al., 1993; Stolzenbach, 1993; Zimmermann-Timm, 2002). This could to some extent contribute to the larger error bars detected in the first stage.

4.3 | From quiescent to turbulent conditions

Compared with the quiescent settling condition, turbulent flows are most likely to be encountered in reality. In real river conditions, inherent properties of microparticles (e.g., density, shape, and size) and hydrodynamic conditions govern the trajectory of nano- and microparticles (Haberstroh et al., 2021; Hoellein et al., 2019; Isachenko, 2020; Vincent & Hoellein, 2021; Waldschläger & Schüttrumpf, 2019). For colloids like SiDNAFe MPs with a larger-than-water density, the sinking rate was likely controlled by the aggregation rates and the shear flow (Quik et al., 2015). Colloidal masses could stay stable in a certain range of shear rates, but could aggregate at higher and lower shear rates (van de Ven & Mason, 1977). Besides, vertical mixing could also be a significant factor determining the probability of particles hitting each other (McNair et al., 1997). Under turbulent flows where more mixing occurs at higher shear velocities, rapid vertical transport would occur, resulting in a more uniform vertical distribution of particles (Ballent et al., 2012). In this regard, increased mixing and cross-sectional particle exchange would probably delay the downstream transport or detain microparticles (Frei et al., 2019; Haberstroh et al., 2021). Moreover, microparticles suspended in near-bed flows are affected by the bed geometry (Phillips et al., 2019). Such microparticles could be easily transferred from the near-bed flows into bed sediments due to a local increase in pressure driven flow into and out of the porous bed (Packman et al., 2000). Under laminar flow conditions, SiDNAFe MPs would have a vertical velocity due to the gravity-driven settling in a similar fashion as in quiescent conditions (Hamm et al., 2011). SiDNAFe MPs would likely be transported downstream as the concentration in the water column depleted gradually due to the gravity-driven settling (Kumar et al., 2021).

Experimental studies on settling and deposition in running rivers and streams originally focused on the cycling of particulate nutrients, such as phosphorus (Newbold et al., 1981, 1983) and fine and coarse particulate organic matter (Paul & Hall, 2002; Wanner & Pusch, 2000). Their findings suggested that as particles move downstream they will decline exponentially with time or longitudinal transport distance. A dimensionless velocity *W* was defined as the ratio of the effective settling velocity observed in a given flow, to that expected in still water. Thus, values of $W > 1$ indicate 'enhanced' settling, and $W < 1$ diminished settling (Hamm et al., 2011). The value of W varies according to particle size, and the factors which affect particle deposition in flowing waters can be interpreted according to the relative influence of gravity and particle momentum (Hoellein et al., 2019).

Current spatio-temporally explicit transport modelling of nano- and micro-particles in rivers utilized the Stokes' settling velocity in still water to model the sedimentation/deposition process (Lazar et al., 2010; Nizzetto et al., 2016). Taking into account the effect of

aggregation on the settling, the concentration profiles of environmental nanomaterials were not so different from the one which did not (Quik et al., 2015). In any case of enhanced or diminished settling during transport in real rivers, we think that the longitudinal concentration profile of SiDNAFe would likely remain comparable to what has been measured for quiescent settling, that is, an exponential-like distribution of SiDNAFe MPs for transport times and distances (Battin et al., 2009; McNair & Newbold, 2012). For the sake of applications of such DNA tracers in future field tracing experiments, the implication of such settling experiment lies in understanding to what extent SiDNAFe MPs would interact with the surroundings and thus remain suspended until the sampling point. Since the settling of such heavier-than-water microparticles of DNA tracers is deemed to happen, but -as observed- not substantially, based on our settling results, a predefined mass loss rate of first-order should be inserted in the mass transport equation (e.g., advection-dispersion-transient storage), for modelling transport of SiDNAFe MPs in real world tracing experiments. As an example, we used an exponential settling function to fit the averaged settling data (ESM in Figure 4d), and arrived at a decay rate of 0.038 per hour for the best-fit case ($R^2 = 0.96$). Besides, there is no significant difference between the ESM fitted curve and the observed averaged curve at 95% significance level ($p > 0.05$).

4.4 | Data uncertainty of DNA analysis

The relatively large error bars across all experiments were due to random variations of qPCR readings, differences per sample in effect of inhibitors, and dilution issues. The first can account for ~±20% of mass variations, and has been widely recognized and discussed in previously published research papers on DNA-based tracers (Mikutis et al., 2018; Tang et al., 2021). With regard to the second, in our qPCR lab, we optimized the protocol so that the trade-off was minimized between diluting the inhibitors and consuming too much time for the labour-intensive washing and up-concentration. Preliminary tests showed that much larger differences existed among replicates when SiDNAFe MPs with lower concentration were exposed to river waters, especially Strijbeek water. Further, the 10-fold dilution series which was used to transform Cq to the mass concentration, was more reliable and reproducible after washing and up-concentrating the SiDNAFe MPs with MQ. Although qPCR theoretically allows the detection of one DNA molecule (Watson et al., 1992), in practice, there is a range of minimal DNA concentrations which is acceptable to be used as initial concentrations to obtain reliable amplifications. The initial concentration chosen for the settling experiments was the middle point between the highest and the lowest measured concentrations.

5 | CONCLUSIONS

In quiescent conditions, more than 60% of SiDNAFe MPs settled within 30 h, which started with a rapid settling phase followed by an exponential-like slow settling phase in the three river waters we used (Meuse, Merkske, and Strijbeek) plus MilliQ water. $D_{h\text{-}DLS}$ of SiDNAFe increased over time, with its PDI positively correlated with the particle size, in suspensions with a 1000× higher particle concentration. From these observations, we inferred that the rapid SiDNAFe settling was mainly due to homo-aggregation and not due to hetero-aggregation (e.g., with particulate matter present in these river waters). Incorporating a first-order mass loss term in the order of 0.038 per hour, which mimics the exponential phase of the settling in quiescent conditions seemed an adequate step forward when modelling the transport of SiDNAFe MPs in river injection experiments. Magnetic separation and up-concentration of superparamagnetic DNA-tagged microparticles in real river waters is a valid and reproducible approach, which is an important advantage for carrying out field-scale tracing experiments. This research adds to the current knowledge of a novel SiDNAFe hydrological colloidal tracer in terms of their settling behaviour and interacting potential with surroundings of similar river conditions, providing insights for future development of a DNA-based tracing framework for hydrological purposes.

ACKNOWLEDGEMENTS

Financial support was provided by the Netherlands Organisation for Scientific Research (NWO) Grant STW14515 WaterTagging and by China Scholarship Council (CSC). We would like to thank Dr. Ahmed Ragab Abdelrady Mahmoud, Dr. Wang Zhengwu, and PhD student Swagatam Chakraborty and Jia Tianlong for their input and fruitful scientific discussions. We would like to thank the lab staff from TUDelft Waterlab, IHE Delft, and De Botanische Tuin for their technical and laboratory support.

DATA AVAILABILITY STATEMENT

The data that support the findings of this study are available from the corresponding author upon reasonable request.

ORCID

Yuchen Tang https://orcid.org/0000-0002-1632-4339

REFERENCES

Abe, T., Kobayashi, S., & Kobayashi, M. (2011). Aggregation of colloidal silica particles in the presence of fulvic acid, humic acid, or alginate: Effects of ionic composition. *Colloids and Surfaces A: Physicochemical and Engineering Aspects*, *379*(1–3), 21–26. https://doi.org/10.1016/j.colsurfa.2010.11.052

Baalousha, M., Cornelis, G., Kuhlbusch, T. A. J., Lynch, I., Nickel, C., Peijnenburg, W., & van den Brink, N. W. (2016). Modeling nanomaterial fate and uptake in the environment: Current knowledge and future trends. *Environmental Science: Nano*, *3*(2), 323–345. https://doi.org/10.1039/c5en00207a

Ballent, A., Purser, A., de Jesus Mendes, P., Pando, S., & Thomsen, L. (2012). Physical transport properties of marine microplastic pollution. *Biogeosciences Discussions*, *9*(12), 18755–18798.

Battin, T. J., Kammer, F. v.d., Weilhartner, A., Ottofuelling, S., & Hofmann, T. (2009). Nanostructured TiO_2: Transport behavior and effects on aquatic microbial communities under environmental conditions. *Environmental Science and Technology*, *43*(21), 8098–8104. https://doi.org/10.1021/es9017046

Besseling, E., Quik, J. T. K., Sun, M., & Koelmans, A. A. (2017). Fate of nano- and microplastic in freshwater systems: A modeling study. *Environmental Pollution*, *220*, 540–548. https://doi.org/10.1016/j.envpol.2016.10.001

Buffle, J., Wilkinson, K. J., Stoll, S., Filella, M., & Zhang, J. (1998). A generalized description of aquatic colloidal interactions: The three-colloidal component approach. *Environmental Science & Technology*, *32*(19), 2887–2899.

Chakraborty, S., Foppen, J. W., & Schijven, J. F. (2022). Effect of concentration of silica encapsulated ds-DNA colloidal microparticles on their transport through saturated porous media. *Colloids and Surfaces A: Physicochemical and Engineering Aspects*, *651*, 129625.

Dahlke, H. E., Williamson, A. G., Georgakakos, C., Leung, S., Sharma, A. N., Lyon, S. W., & Walter, M. T. (2015). Using concurrent DNA tracer injections to infer glacial flow pathways. *Hydrological Processes*, *29*(25), 5257–5274. https://doi.org/10.1002/hyp.10679

Domingos, R. F., Ju-nam, Y. O. N., Reid, M. M., Tufenkji, N., Lead, J. R., & Leppard, G. G. (2009). Characterizing manufactured nanoparticles in the environment: multimethod determination of particle sizes. *Environmental Science & Technology*, *43*(19), 7277–7284. https://doi.org/10.1021/es900249m

Domingos, R. F., Tufenkji, N., & Wilkinson, K. J. (2009). Aggregation of titanium dioxide nanoparticles: Role of a fulvic acid. *Environmental Science & Technology*, *43*(5), 1282–1286.

Elimelech, M., Gregory, J., & Jia, X. (2013). *Particle deposition and aggregation: Measurement, modelling and simulation*. Butterworth-Heinemann.

Foppen, J. W., Seopa, J., Bakobie, N., & Bogaard, T. (2013). Development of a methodology for the application of synthetic DNA in stream tracer injection experiments. *Water Resources Research*, *49*(9), 5369–5380. https://doi.org/10.1002/wrcr.20438

Frei, S., Piehl, S., Gilfedder, B. S., Löder, M. G. J., Krutzke, J., Wilhelm, L., & Laforsch, C. (2019). Occurence of microplastics in the hyporheic zone of rivers. *Scientific Reports*, *9*(1), 1–11.

Garner, K. L., Suh, S., & Keller, A. A. (2017). Assessing the risk of engineered nanomaterials in the environment: Development and application of the nanoFate model. *Environmental Science & Technology*, *51*(10), 5541–5551.

Garnett, M. C., Ferruti, P., Ranucci, E., Suardi, M. A., Heyde, M., & Sleat, R. (2009). Sterically stabilized self-assembling reversibly cross-linked polyelectrolyte complexes with nucleic acids for environmental and medical applications. *Biochemical Society Transactions*, *37*(4), 713–716. https://doi.org/10.1042/BST0370713

Haberstroh, C. J., Arias, M. E., Yin, Z., & Wang, M. C. (2021). Effects of hydrodynamics on the cross-sectional distribution and transport of plastic in an urban coastal river. *Water Environment Research*, *93*(2), 186–200. https://doi.org/10.1002/wer.1386

Hamm, N. T., Dade, W. B., & Renshaw, C. E. (2011). Fine particle deposition to porous beds. *Water Resources Research*, *47*(11), W11508. https://doi.org/10.1029/2010WR010295

Hochella, M. F., Jr., Mogk, D. W., Ranville, J., Allen, I. C., Luther, G. W., Marr, L. C., McGrail, B. P., Murayama, M., Qafoku, N. P., & Rosso, K. M. (2019). Natural, incidental, and engineered nanomaterials and their impacts on the earth system. *Science*, *363*(6434), eaau8299.

Hoellein, T. J., Shogren, A. J., Tank, J. L., Risteca, P., & Kelly, J. J. (2019). Microplastic deposition velocity in streams follows patterns for naturally occurring allochthonous particles. *Scientific Reports*, *9*(1), 3740. https://doi.org/10.1038/s41598-019-40126-3

Holland, J. H. (1992). Genetic algorithms. *Scientific American*, *267*(1), 66–73. https://doi.org/10.2307/24939139

Hünken, A., & Mutz, M. (2007). Field studies on factors affecting very fine and ultra fine particulate organic matter deposition in low-gradient sand-bed streams. *Hydrological Processes*, *21*(4), 525–533. https://doi.org/10.1002/hyp.6263

Isachenko, I. (2020). Catching the variety: Obtaining the distribution of terminal velocities of microplastics particles in a stagnant fluid by a stochastic simulation. *Marine Pollution Bulletin*, *159*, 111464. https://doi.org/10.1016/j.marpolbul.2020.111464

Jekel, M. R. (1986). The stabilization of dispersed mineral particles by adsorption of humic substances. *Water Research*, *20*(12), 1543–1554.

Jerry, O., & Pecoraro, J. (1996). Electrophoretic mobility of cryptosporidium oocysts and giardia cysts. *Journal of Environmental Engineering*, *122*(3), 228–231. https://doi.org/10.1061/(ASCE)0733-9372(1996)122:3(228)

Johnson, C. P., Li, X., & Logan, B. E. (1996). Settling velocities of fractal aggregates. *Environmental Science & Technology*, *30*(6), 1911–1918.

Khelifa, A., & Hill, P. S. (2006). Models for effective density and settling velocity of flocs. *Journal of Hydraulic Research*, *44*(3), 390–401.

Kim, J. Y., & Sansalone, J. J. (2008). Zeta potential of clay-size particles in urban rainfall-runoff during hydrologic transport. *Journal of Hydrology*, *356*(1–2), 163–173. https://doi.org/10.1016/j.jhydrol.2008.04.006

Klaine, S. J., Alvarez, P. J., Batley, G. E., Fernandes, T. F., Handy, R. D., Lyon, D. Y., Mahendra, S., McLaughlin, M. J., & Lead, J. R. (2008). Nanomaterials in the environment: Behavior, fate, bioavailability, and effects. *Environmental Toxicology and Chemistry: An International Journal*, *27*(9), 1825–1851.

Kooi, M., Besseling, E., Kroeze, C., van Wezel, A. P., & Koelmans, A. A. (2018). Modeling the fate and transport of plastic debris in freshwaters: Review and guidance. In M. Wagner & S. Lambert (Eds.), *Freshwater microplastics: Emerging environmental contaminants?* (pp. 125–152). Springer International Publishing. https://doi.org/10.1007/978-3-319-61615-5_7

Koppel, D. E. (1972). Analysis of macromolecular polydispersity in intensity correlation spectroscopy: The method of cumulants. *The Journal of Chemical Physics*, *57*(11), 4814–4820.

Kumar, R., Sharma, P., Verma, A., Jha, P. K., Singh, P., Gupta, P. K., Chandra, R., & Vara Prasad, P. V. (2021). Effect of physical characteristics and hydrodynamic conditions on transport and deposition of microplastics in riverine ecosystem. *Water*, *13*(19), 2710. https://doi.org/10.3390/w13192710

Labille, J., Harns, C., Bottero, J.-Y., & Brant, J. (2015). Heteroaggregation of titanium dioxide nanoparticles with natural clay colloids. *Environmental Science & Technology*, *49*, 6608–6616. https://doi.org/10.1021/acs.est.5b00357

Lagarde, F., Olivier, O., Zanella, M., Daniel, P., Hiard, S., & Caruso, A. (2016). Microplastic interactions with freshwater microalgae: Heteroaggregation and changes in plastic density appear strongly dependent on polymer type. *Environmental Pollution*, *215*, 331–339.

Larsen, L. G., Harvey, J. W., Noe, G. B., & Crimaldi, J. P. (2009). Predicting organic floc transport dynamics in shallow aquatic ecosystems: Insights from the field, the laboratory, and numerical modeling. *Water Resources Research*, *45*(1), W01411.

Lartiges, B. S., Deneux-Mustin, S., Villemin, G., Mustin, C., Barres, O., Chamerois, M., Gerard, B., & Babut, M. (2001). Composition, structure and size distribution of suspended particulates from the Rhine River. *Water Research*, *35*(3), 808–816.

Lazar, A. N., Butterfield, D., Futter, M. N., Rankinen, K., Thouvenot-Korppoo, M., Jarritt, N., Lawrence, D. S. L., Wade, A. J., & Whitehead, P. G. (2010). An assessment of the fine sediment dynamics in an upland river system: INCA-sed modifications and implications for fisheries. *Science of the Total Environment*, *408*(12), 2555–2566.

Lead, J. R., Batley, G. E., Alvarez, P. J., Croteau, M. N., Handy, R. D., McLaughlin, M. J., Judy, J. D., & Schirmer, K. (2018). Nanomaterials in the environment: Behavior, fate, bioavailability, and effects—An updated review. *Environmental Toxicology and Chemistry*, *37*(8), 2029–2063.

Lee, B. J., Kim, J., Hur, J., Choi, I. H., Toorman, E. A., Fettweis, M., & Choi, J. W. (2019). Seasonal dynamics of organic matter composition and its effects on suspended sediment flocculation in river water. *Water Resources Research*, *55*(8), 6968–6985. https://doi.org/10.1029/2018WR024486

Leibundgut, C., & Seibert, J. (2011). Tracer hydrology. *Treatise on Water Science*, *2*, 215–236. https://doi.org/10.1016/B978-0-444-53199-5.00036-1

Lerche, D. (2002). Dispersion stability and particle characterization by sedimentation kinetics in a centrifugal field. *Journal of Dispersion Science and Technology*, *23*(5), 699–709. https://doi.org/10.1081/DIS-120015373

Liao, R., Zhang, J., Li, T., Luo, D., & Yang, D. (2020). Biopolymer/plasmid DNA microspheres as tracers for multiplexed hydrological investigation. *Chemical Engineering Journal*, *401*, 401. https://doi.org/10.1016/j.cej.2020.126035

Lick, W., Huang, H., & Jepsen, R. (1993). Flocculation of fine-grained sediments due to differential settling. *Journal of Geophysical Research*, *98*(C6), 10279. https://doi.org/10.1029/93jc00519

Liu, X., Wazne, M., Chou, T., Xiao, R., & Xu, S. (2011). Influence of Ca^{2+} and Suwannee River humic acid on aggregation of silicon nanoparticles in aqueous media. *Water Research*, *45*(1), 105–112.

Li, Y., Wang, X., Fu, W., Xia, X., Liu, C., Min, J., Zhang, W., & Crittenden, J. C. (2019). Interactions between nano/micro plastics and suspended sediment in water: Implications on aggregation and settling. *Water Research*, *161*, 486–495. https://doi.org/10.1016/j.watres.2019.06.018

Maggi, F., & Tang, F. H. M. (2015). Analysis of the effect of organic matter content on the architecture and sinking of sediment aggregates. *Marine Geology*, *363*, 102–111. https://doi.org/10.1016/j.margeo.2015.01.017

Mahler, B. J., Matthew, W., Philip, B., & Hillis, D. M. (1998). DNA-labeled clay: A sensitive new method for tracing particle transport. *Geology*, *26*(9), 831–834.

Malm, A. V., & Corbett, J. C. (2019). Improved dynamic light scattering using an adaptive and statistically driven time resolved treatment of correlation data. *Scientific Reports*, *9*(1), 1–11.

Many, G., Bourrin, F., de Madron, X. D., Pairaud, I., Gangloff, A., Doxaran, D., Ody, A., Verney, R., Menniti, C., & le Berre, D. (2016). Particle assemblage characterization in the Rhone River ROFI. *Journal of Marine Systems*, *157*, 39–51.

Ma, S., Zhou, K., Yang, K., & Lin, D. (2015). Heteroagglomeration of oxide nanoparticles with algal cells: Effects of particle type, ionic strength and pH. *Environmental Science & Technology*, *49*(2), 932–939.

McNair, J. N., & Newbold, J. D. (2012). Turbulent particle transport in streams: Can exponential settling be reconciled with fluid mechanics? *Journal of Theoretical Biology*, *300*, 62–80. https://doi.org/10.1016/j.jtbi.2012.01.016

McNair, J. N., Newbold, J. D., & Hart, D. D. (1997). Turbulent transport of suspended particles and dispersing benthic organisms: How long to hit bottom? *Journal of Theoretical Biology*, *188*(1), 29–52.

McNew, C. P., Wang, C., Walter, M. T., & Dahlke, H. E. (2018). Fabrication, detection, and analysis of DNA-labeled PLGA particles for environmental transport studies. *Journal of Colloid and Interface Science*, *526*, 207–219. https://doi.org/10.1016/j.jcis.2018.04.059

Metin, C. O., Bonnecaze, R. T., Lake, L. W., Miranda, C. R., & Nguyen, Q. P. (2014). Aggregation kinetics and shear rheology of aqueous silica suspensions. *Applied Nanoscience*, *4*(2), 169–178. https://doi.org/10.1007/s13204-012-0185-6

Mikutis, G., Deuber, C. A., Schmid, L., Kittilä, A., Lobsiger, N., Puddu, M., Asgeirsson, D. O., Grass, R. N., Saar, M. O., & Stark, W. J. (2018). Silica-encapsulated DNA-based tracers for aquifer characterization. *Environmental Science & Technology*, *52*(21), 12142–12152.

Morrison, I. D., Grabowski, E. F., & Herb, C. A. (1985). Improved techniques for particle size determination by quasi-elastic light scattering. *Langmuir*, *1*, 496–501. https://doi.org/10.1021/la00064a016

Newbold, J. D., Elwood, J. W., O'Neill, R. V., & Sheldon, A. L. (1983). Phosphorus dynamics in a woodland stream ecosystem: A study of nutrient spiralling. *Ecology*, *64*(5), 1249–1265.

Newbold, J. D., Elwood, J. W., O'Neill, R. V., & Winkle, W. V. (1981). Measuring nutrient spiralling in streams. *Canadian Journal of Fisheries and Aquatic Sciences*, *38*(7), 860–863.

Newbold, J. D., Thomas, S. A., Minshall, G. W., Cushing, C. E., & Georgian, T. (2005). Deposition, benthic residence, and resuspension of fine organic particles in a mountain stream. *Limnology and Oceanography*, *50*(5), 1571–1580.

Nizzetto, L., Bussi, G., Futter, M. N., Butterfield, D., & Whitehead, P. G. (2016). A theoretical assessment of microplastic transport in river catchments and their retention by soils and river sediments. *Environmental Science: Processes and Impacts*, *18*(8), 1050–1059. https://doi.org/10.1039/c6em00206d

Oncsik, T., Trefalt, G., Csendes, Z., Szilagyi, I., & Borkovec, M. (2014). Aggregation of negatively charged colloidal particles in the presence of multivalent cations. *Langmuir*, *30*(3), 733–741. https://doi.org/10.1021/la4046644

Ongley, E. D., Krishnappan, B. G., Droppo, G., Rao, S. S., & Maguire, R. J. (1992). Cohesive sediment transport: Emerging issues for toxic chemical management. *Hydrobiologia*, *235*(1), 177–187.

Ottofuelling, S., von der Kammer, F., & Hofmann, T. (2011). Commercial titanium dioxide nanoparticles in both natural and synthetic water: Comprehensive multidimensional testing and prediction of aggregation behavior. *Environmental Science and Technology*, *45*(23), 10045–10052. https://doi.org/10.1021/es2023225

Packman, A. I., Brooks, N. H., & Morgan, J. J. (2000). A physicochemical model for colloid exchange between a stream and a sand streambed with bed forms. *Water Resources Research*, *36*(8), 2351–2361.

Pang, L., Abeysekera, G., Hanning, K., Premaratne, A., Robson, B., Abraham, P., Sutton, R., Hanson, C., Hadfield, J., Heiligenthal, L., Stone, D., McBeth, K., & Billington, C. (2020). Water tracking in surface water, groundwater and soils using free and alginate-chitosan encapsulated synthetic DNA tracers. *Water Research*, *184*, 184. https://doi.org/10.1016/j.watres.2020.116192

Paul, M. J., & Hall, R. O., Jr. (2002). Particle transport and transient storage along a stream-size gradient in the Hubbard Brook Experimental Forest. *Journal of the North American Benthological Society*, *21*(2), 195–205.

Paunescu, D., Puddu, M., Soellner, J. O. B., Stoessel, P. R., & Grass, R. N. (2013). Reversible DNA encapsulation in silica to produce ROS-resistant and heat-resistant synthetic DNA "fossils". *Nature Protocols*, *8*(12), 2440–2448. https://doi.org/10.1038/nprot.2013.154

Petosa, A. R., Jaisi, D. E. B. P., Quevedo, I. R., Elimelech, M., & Tufenkji, N. (2010). Aggregation and deposition of engineered nanomaterials in aquatic environments: Role of physicochemical interactions. *Environmental Science & Technology*, *44*(17), 6532–6549.

Phillips, C. B., Dallmann, J. D., Jerolmack, D. J., & Packman, A. I. (2019). Fine-particle deposition, retention, and resuspension within a sand-bedded stream are determined by streambed morphodynamics. *Water Resources Research*, *55*, 303–318. https://doi.org/10.1029/2019wr025272

Praetorius, A., Badetti, E., Brunelli, A., Clavier, A., Gallego-Urrea, J. A., Gondikas, A., Hassellöv, M., Hofmann, T., Mackevica, A., & Marcomini, A. (2020). Strategies for determining heteroaggregation attachment efficiencies of engineered nanoparticles in aquatic environments. *Environmental Science: Nano*, *7*(2), 351–367.

Praetorius, A., Scheringer, M., & Hungerbühler, K. (2012). Development of environmental fate models for engineered nanoparticles – A case study of TiO_2 nanoparticles in the Rhine River. *Environmental Science & Technology*, *46*(12), 6705–6713.

Puddu, M., Paunescu, D., Stark, W. J., & Grass, R. N. (2014). Magnetically recoverable, thermostable, hydrophobic DNA/silica encapsulates and their application as invisible oil tags. *ACS Nano*, *8*(3), 2677–2685. https://doi.org/10.1021/nn4063853

Quik, J. T. K., de Klein, J. J. M., & Koelmans, A. A. (2015). Spatially explicit fate modelling of nanomaterials in natural waters. *Water Research*, *80*, 200–208. https://doi.org/10.1016/j.watres.2015.05.025

Quik, J. T. K., Lynch, I., van Hoecke, K., Miermans, C. J. H., de Schamphelaere, K. A. C., Janssen, C. R., Dawson, K. A., Cohen, M. A., & van de Meent, D. (2010). Chemosphere effect of natural organic matter on cerium dioxide nanoparticles settling in model fresh water. *Chemosphere*, *81*(6), 711–715. https://doi.org/10.1016/j.chemosphere.2010.07.062

Quik, J. T. K., Stuart, M. C., Wouterse, M., Peijnenburg, W., Hendriks, A. J., & van de Meent, D. (2012). Natural colloids are the dominant factor in the sedimentation of nanoparticles. *Environmental*

Toxicology and Chemistry, *31*(5), 1019–1022. https://doi.org/10.1002/etc.1783

Quik, J. T. K., Velzeboer, I., Wouterse, M., & Koelmans, A. A. (2013). Heteroaggregation and sedimentation rates for nanomaterials in natural waters. *Water Research*, *48*, 269–279. https://doi.org/10.1016/j.watres.2013.09.036

Sabir, I. H., Torgersen, J., Haldorsen, S., & Aleström, P. (1999). DNA tracers with information capacity and high detection sensitivity tested in groundwater studies. *Hydrogeology Journal*, *7*(3), 264–272. https://doi.org/10.1007/s100400050200

Sharma, A., Foppen, J. W., Banerjee, A., Sawssen, S., Bachhar, N., Peddis, D., & Bandyopadhyay, S. (2021). Magnetic nanoparticles to unique DNA tracers: Effect of functionalization on physico-chemical properties. *Nanoscale Research Letters*, *16*(1), 24. https://doi.org/10.1186/s11671-021-03483-5

Sharma, A. N., Luo, D., & Walter, M. T. (2012). Hydrological tracers using nanobiotechnology: Proof of concept. *Environmental Science and Technology*, *46*(16), 8928–8936. https://doi.org/10.1021/es301561q

Shevlin, D., O'Brien, N., & Cummins, E. (2018). Silver engineered nanoparticles in freshwater systems – Likely fate and behaviour through natural attenuation processes. *Science of the Total Environment*, *621*, 1033–1046. https://doi.org/10.1016/j.scitotenv.2017.10.123

Slomberg, D. L., Ollivier, P., Radakovitch, O., Baran, N., Sani-Kast, N., Miche, H., Borschneck, D., Grauby, O., Bruchet, A., & Scheringer, M. (2016). Characterisation of suspended particulate matter in the Rhone River: Insights into analogue selection. *Environmental Chemistry*, *13*(5), 804–815.

Stokes, G. G. (1850). On the effect of internal friction of fluids on the motion of pendulums. *Transactions of the Cambridge Philosophical Society*, *9*(8), 106.

Stolzenbach, K. D. (1993). Scavenging of small particles by fast-sinking porous aggregates. *Deep Sea Research Part I: Oceanographic Research Papers*, *40*(2), 359–369.

Stetefeld, J., McKenna, S. A., & Patel, T. R. (2016). Dynamic light scattering: A practical guide and applications in biomedical sciences. *Biophysical Reviews*, *8*(4), 409–427.

Tang, F. H. M., & Maggi, F. (2016). A mesocosm experiment of suspended particulate matter dynamics in nutrient-and biomass-affected waters. *Water Research*, *89*, 76–86.

Tang, Y., Foppen, J. W., & Bogaard, T. A. (2021). Transport of silica encapsulated DNA microparticles in controlled instantaneous injection open channel experiments. *Journal of Contaminant Hydrology*, *242*, 242. https://doi.org/10.1016/j.jconhyd.2021.103880

van de Ven, T. G. M., & Mason, S. G. (1977). The mierorheology of colloidal dispersions. *Colloid & Polymer Science*, *255*(8), 794–804.

van Emmerik, T., & Schwarz, A. (2020). Plastic debris in rivers. *Wiley Interdisciplinary Reviews: Water*, *7*(1), 1–24. https://doi.org/10.1002/wat2.1398

van Emmerik, T., Strady, E., Kieu-Le, T. C., Nguyen, L., & Gratiot, N. (2019). Seasonality of riverine macroplastic transport. *Scientific Reports*, *9*(1), 13549. https://doi.org/10.1038/s41598-019-50096-1

Velde, B. (1977). *Clays and clay minerals in natural and synthetic systems*. Elsevier.

Velzeboer, I., Quik, J. T. K., van de Meent, D., & Koelmans, A. A. (2014). Rapid settling of nanoparticles due to heteroaggregation with suspended sediment. *Environmental Toxicology and Chemistry*, *33*(8), 1766–1773. https://doi.org/10.1002/etc.2611

Vincent, A. E. S., & Hoellein, T. J. (2021). Distribution and transport of microplastic and fine particulate organic matter in urban streams. *Ecological Applications*, *31*(8), e02429. https://doi.org/10.1002/eap.2429

Waldschläger, K., & Schüttrumpf, H. (2019). Effects of particle properties on the settling and rise velocities of microplastics in freshwater under laboratory conditions. *Environmental Science and Technology*, *53*(4), 1958–1966. https://doi.org/10.1021/acs.est.8b06794

Wanner, S. C., & Pusch, M. (2000). Use of fluorescently labeled lycopodium spores as a tracer for suspended particles in a lowland river. *Journal of the North American Benthological Society*, *19*(4), 648–658.

Watson, J. D., Gilman, M., Witkowski, J., & Genentech, I. (1992). *Recombinant DNA*. Macmillan.

Wilson, M. J., Wilson, L., Patey, I., & Shaw, H. (2014). The influence of individual clay minerals on formation damage of reservoir sandstones: A critical review with some new insights. *Clay Minerals*, *49*(2), 147–164.

Zhang, Y., Chen, Y., Westerhoff, P., & Crittenden, J. (2009). Impact of natural organic matter and divalent cations on the stability of aqueous nanoparticles. *Water Research*, *43*(17), 4249–4257.

Zhao, J., Li, Y., Wang, X., Xia, X., Shang, E., & Ali, J. (2021). Ionic-strength-dependent effect of suspended sediment on the aggregation, dissolution and settling of silver nanoparticles. *Environmental Pollution*, *279*, 279. https://doi.org/10.1016/j.envpol.2021.116926

Zhu, B., Xia, X., Zhang, S., & Tang, Y. (2018). Attenuation of bacterial cytotoxicity of carbon nanotubes by riverine suspended solids in water. *Environmental Pollution*, *234*, 581–589. https://doi.org/10.1016/j.envpol.2017.11.086

Zimmermann-Timm, H. (2002). Characteristics, dynamics and importance of aggregates in rivers – An invited review. *International Review of Hydrobiology*, *87*(2–3), 197–240.

SUPPORTING INFORMATION

Additional supporting information can be found online in the Supporting Information section at the end of this article.

How to cite this article: Tang, Y., Zhang, F., Bogaard, T., Chassagne, C., Ali, Z., Bandyopadhyay, S., & Foppen, J. W. (2023). Settling of superparamagnetic silica encapsulated DNA microparticles in river water. *Hydrological Processes*, *37*(1), e14801. https://doi.org/10.1002/hyp.14801